

On the prevalence of early mass transfer for very massive binaries

C. A. BURT,¹ M. RENZO,¹ A. GRICHENER,¹ AND ■ [TBD] ■

¹ *University of Arizona, Department of Astronomy & Steward Observatory, 933 N. Cherry Ave., Tucson, AZ 85721, USA*

ABSTRACT

Common phases of mass transfer in stellar binaries are case A (during the donor’s main sequence) and case B (after the donor’s main sequence but before helium core depletion). Most stars see stellar radii significantly grow after the main sequence, making case B more common. However, very massive stars may already undergo significant expansion during the main sequence increasing the probability of case A mass transfer. We find that using convective boundary mixing informed by the width of the main sequence in 30 Doradus, case A mass transfer dominates for donor masses $\gtrsim 75 M_{\odot}$. This is not the case without convective boundary mixing or in the stellar models commonly used in rapid binary population synthesis. Therefore, case A mass transfer may be more dominant than commonly assumed, with potential impact on rates of all post mass transfer binaries, from Wolf-rayet-O-type binaries, to X-ray binaries, and gravitational wave progenitors.

1. MASS TRANSFER IN VERY MASSIVE BINARIES

Binary stars with a sufficiently small orbital separation ($a \lesssim 2500 R_{\odot}$, e.g. Sana et al. 2012) undergo (at least one) mass transfer phases in which the donor star transfers mass to the initially less massive accretor. For very massive stars ($\gtrsim 30 M_{\odot}$), mass transfer most often occurs during the donor’s hydrogen core-burning (case A) or helium core-burning (case B), which together account for $\sim 99\%$ of the donor’s lifetime (Kippenhahn & Weigert 1967).

For a flat in $\log_{10}(a)$ initial separation distribution (Öpik 1924), case B is expected to occur more often than case A mass transfer, since most stars expand dramatically post-main sequence (e.g., van den Heuvel 1969). However, very massive stars may already undergo a drastic expansion in radius during their main sequence (e.g., Sanyal et al. 2015; Jiang et al. 2015). This may increase the rate of case A (de Mink et al. 2008), affecting the evolution of the star and consequently potentially altering stellar parameters that determine the rate of Wolf-Rayet+O-type binaries (e.g., Nuijten & Nelemans 2024), and X-ray binaries and gravitational wave progenitors (e.g., Mandel & Broekgaarden 2022).

The radius of the donor is dependent on poorly constrained stellar parameters, including stellar winds (Renzo et al. 2017; Josiek et al. 2024), metallicity (Xin et al. 2022), treatment of close-to-super-Eddington-layers (e.g., Joss et al. 1973; Paxton et al. 2013; Jiang et al. 2015; Agrawal et al. 2022; Jermyn et al. 2023), and convective boundary mixing (Anders & Pedersen 2023;

Johnston et al. 2024). We explore the radial evolution of very massive stars while varying convective boundary mixing and metallicity with models commonly adopted in rapid binary population synthesis.

2. COMPARING DONOR RADII

We computed MESA models¹ (version 24.03.1, Paxton et al. 2011, 2013, 2015, 2018, 2019; Jermyn et al. 2023) from $30 M_{\odot}$ to $100 M_{\odot}$ in steps of $5 M_{\odot}$ at metallicity $Z = 0.001$ and 0.0001 following the setup from Renzo et al. (2023). The gray lines in Fig. 1 show their radial evolution as a function of time.

We explore models with (top panel) and without overshooting (middle panel) and compare them to the Pols et al. (1998) models (bottom panel) used in SSE (Hurley et al. 2000) generated using COMPAS (Stevenson et al. 2017; Vigna-Gómez et al. 2018; Riley et al. 2022), which is extrapolated for masses $\geq 50 M_{\odot}$.

When using overshooting, our MESA models implement an exponential algorithm (Herwig 2000) fit to the step overshooting calibrated on the width of main sequence in 30 Doradus (~ 0.335 pressure scale heights, Brott et al. 2011) following Claret & Torres (2018), corresponding to $(f, f_0) = (0.0415, 0.008)$. This relatively “large overshooting” model is compared to models not including any convective boundary mixing, and to the Pols et al. (1998) models including an effectively mass-dependent overshooting. The red and blue dashed lines in each panel of Fig. 1 denote the maxi-

¹ Publicly available at doi.org/10.5281/zenodo.14757819

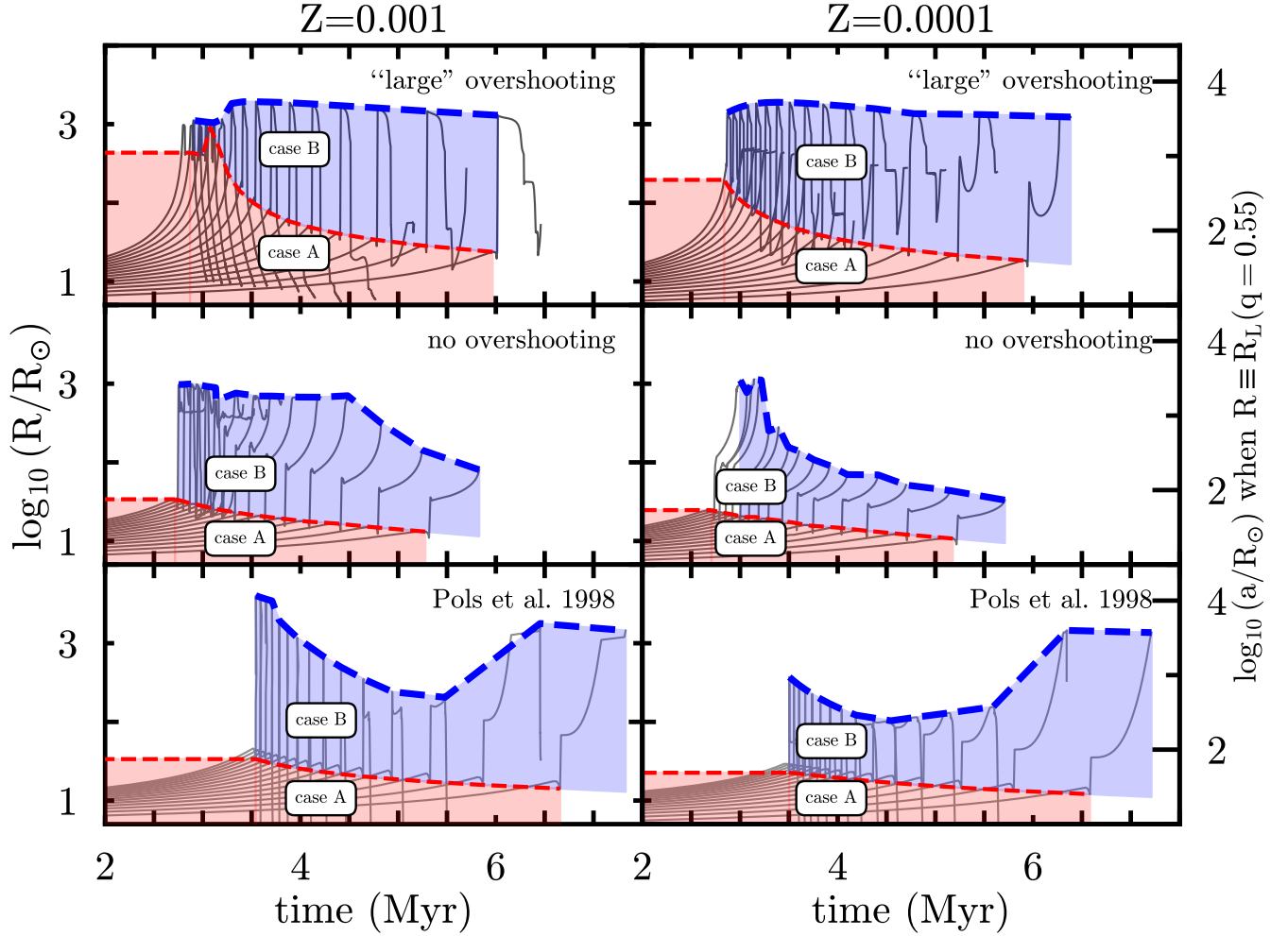


Figure 1. Each panel contain 15 stellar MESA models spanning from $30 M_{\odot}$ star (longer lifetimes) to $100 M_{\odot}$ (shorter lifetimes). The top panels show models with [Brott et al. \(2011\)](#)-like convective boundary mixing (“large” overshooting), the middle show models without overshooting, and the bottom panels plot models generated from COMPAS based on analytic fits to the stellar models of [Pols et al. \(1998\)](#). The left (right) panels have a metallicity $Z = 0.001$ ($Z = 0.0001$). Dashed red (blue) lines mark the maximum radius during the main sequence (during the runtime of the model). The red (blue) shaded areas underneath correspond to case A (case B) mass transfer.

maximum radius during the main sequence and helium core burning phase, respectively. These mark the maximum Roche radius for a case A and case B donor, respectively. The right axis shows orbital separations a where the stellar radius meets the roche radius computed from [Eggleton \(1983\)](#), assuming a representative accretor-to-donor mass ratio of $q = 0.55$. This value corresponds to the average for a flat mass-ratio distribution between 0.1 and 1 ([Kobulnicky & Fryer 2007](#); [Sana et al. 2012](#)). The red regions denote binaries which will undergo case A mass transfer and the blue regions denote binaries which will undergo case B mass transfer. For $Z = 0.001$, when including overshooting (top left panel), donors with masses $\gtrsim 75 M_{\odot}$ overwhelmingly experience case A. Removing convective boundary mixing (middle)

keeps main sequence radii smaller, preserving the blue region above the red line for case B mass transfer at all masses. The overshooting implementation from [Pols et al. \(1998\)](#) (bottom), while nonzero, still leaves a large window for case B up to at least $100 M_{\odot}$. At even lower metallicities of $Z = 0.0001$ (right), stars are more compact, and all models allow for case B mass transfer at all masses.

3. IMPLICATIONS FOR POST-MASS-TRANSFER BINARIES

Convective boundary mixing ([Brott et al. 2011](#); [Johnston et al. 2024](#)) and metallicity have a strong effect on stellar radii, which determine when a donor fills its Roche lobe. Related effects on stellar radii have been explored elsewhere, including the adopted wind mass loss

rates (e.g., [Smith 2014](#); [Renzo et al. 2017](#); [Josiek et al. 2024](#)), rotation (and consequently tides, e.g., [Maeder & Meynet 2000](#)), and the treatment of energy transport in correspondence of opacity bumps in the envelope (e.g., [Joss et al. 1973](#); [Agrawal et al. 2022](#); [Cheng et al. 2024](#)).

After a thermal-timescale initial phase, Case A mass transfer occurs overall on a longer (nuclear) timescale, while case B occurs entirely on a much shorter (thermal) timescale (but see [Klencki et al. 2022](#)). Moreover, the dynamical stability of the orbit during mass transfer is sensitive to the evolutionary phase of the stars involved (e.g., [Claeys et al. 2014](#)). Therefore, whether a given binary experiences dynamically unstable mass transfer, which is critical to determine the outcome of the binary system, depends on more than just the mass ratio, as generally assumed in rapid population synthesis. Comparing rows in Fig. 1 shows that the stellar evolution models commonly used in rapid population synthesis are qualitatively similar to our no overshooting models, in the sense that they allow for case B mass

transfer in all mass regions we sampled and for metallicities relevant to galactic and gravitational astronomy.

Given the critical role of mass transfer for the formation of many binaries of interest, the fraction of systems experiencing case A in respect to case B may significantly impact predicted rates for post mass transfer binaries, including Wolf-Rayet+O-type binaries, X-ray generated binaries, and gravitational wave progenitors. In particular, the role of the stable mass transfer channel (e.g., [Marchant et al. 2021](#); [van Son et al. 2022](#)) for (massive) binary black hole mergers is currently hotly debated. Our results highlight that stellar uncertainties influence the mode of mass transfer and consequently the outcomes.

Software: This work made use of the following software packages: `matplotlib` ([Hunter 2007](#)) and `python` ([Van Rossum & Drake 2009](#)), <http://github.com/TeamCOMPAS/COMPAS>, and <https://docs.mesastar.org> MESA. Software citation information aggregated using [The Software Citation Station](#) ([Wagg & Broekgaarden 2024](#); [Wagg et al. 2024](#)).

REFERENCES

- Agrawal, P., Stevenson, S., Szécsi, D., & Hurley, J. 2022, *A&A*, 668, A90, doi: [10.1051/0004-6361/202244044](#)
- Anders, E. H., & Pedersen, M. G. 2023, *Galaxies*, 11, 56, doi: [10.3390/galaxies11020056](#)
- Brott, I., de Mink, S. E., Cantiello, M., et al. 2011, *A&A*, 530, A115, doi: [10.1051/0004-6361/201016113](#)
- Cheng, S. J., Goldberg, J. A., Cantiello, M., et al. 2024, *ApJ*, 974, 270, doi: [10.3847/1538-4357/ad701e](#)
- Claeys, J. S. W., Pols, O. R., Izzard, R. G., Vink, J., & Verbunt, F. W. M. 2014, *A&A*, 563, A83, doi: [10.1051/0004-6361/201322714](#)
- Claret, A., & Torres, G. 2018, *ApJ*, 859, 100, doi: [10.3847/1538-4357/aabd35](#)
- de Mink, S. E., Pols, O. R., & Yoon, S. C. 2008, in *American Institute of Physics Conference Series*, Vol. 990, *First Stars III*, ed. B. W. O’Shea & A. Heger (AIP), 230–232, doi: [10.1063/1.2905549](#)
- Eggleton, P. P. 1983, *ApJ*, 268, 368, doi: [10.1086/160960](#)
- Herwig, F. 2000, *A&A*, 360, 952, doi: [10.48550/arXiv.astro-ph/0007139](#)
- Hunter, J. D. 2007, *Computing in Science & Engineering*, 9, 90, doi: [10.1109/MCSE.2007.55](#)
- Hurley, J. R., Pols, O. R., & Tout, C. A. 2000, *MNRAS*, 315, 543, doi: [10.1046/j.1365-8711.2000.03426.x](#)
- Jermyn, A. S., Bauer, E. B., Schwab, J., et al. 2023, *ApJS*, 265, 15, doi: [10.3847/1538-4365/acae8d](#)
- Jiang, Y.-F., Cantiello, M., Bildsten, L., Quataert, E., & Blaes, O. 2015, *ApJ*, 813, 74, doi: [10.1088/0004-637X/813/1/74](#)
- Johnston, C., Michielsen, M., Anders, E. H., et al. 2024, *ApJ*, 964, 170, doi: [10.3847/1538-4357/ad2343](#)
- Josiek, J., Ekström, S., & Sander, A. A. C. 2024, *A&A*, 688, A71, doi: [10.1051/0004-6361/202449281](#)
- Joss, P. C., Salpeter, E. E., & Ostriker, J. P. 1973, *ApJ*, 181, 429, doi: [10.1086/152060](#)
- Kippenhahn, R., & Weigert, A. 1967, *ZA*, 65, 251
- Klencki, J., Istrate, A., Nelemans, G., & Pols, O. 2022, *A&A*, 662, A56, doi: [10.1051/0004-6361/202142701](#)
- Kobulnicky, H. A., & Fryer, C. L. 2007, *ApJ*, 670, 747, doi: [10.1086/522073](#)
- Maeder, A., & Meynet, G. 2000, *ARA&A*, 38, 143, doi: [10.1146/annurev.astro.38.1.143](#)
- Mandel, I., & Broekgaarden, F. S. 2022, *Living Reviews in Relativity*, 25, 1, doi: [10.1007/s41114-021-00034-3](#)
- Marchant, P., Pappas, K. M. W., Gallegos-Garcia, M., et al. 2021, *A&A*, 650, A107, doi: [10.1051/0004-6361/202039992](#)
- Nuijten, M., & Nelemans, G. 2024, *arXiv e-prints*, arXiv:2412.00938, doi: [10.48550/arXiv.2412.00938](#)
- Öpik, E. 1924, *Publications of the Tartu Astrofizika Observatory*, 25, 1
- Paxton, B., Bildsten, L., Dotter, A., et al. 2011, *ApJS*, 192, 3, doi: [10.1088/0067-0049/192/1/3](#)

- Paxton, B., Cantiello, M., Arras, P., et al. 2013, *ApJS*, 208, 4, doi: [10.1088/0067-0049/208/1/4](https://doi.org/10.1088/0067-0049/208/1/4)
- Paxton, B., Marchant, P., Schwab, J., et al. 2015, *ApJS*, 220, 15, doi: [10.1088/0067-0049/220/1/15](https://doi.org/10.1088/0067-0049/220/1/15)
- Paxton, B., Schwab, J., Bauer, E. B., et al. 2018, *ApJS*, 234, 34, doi: [10.3847/1538-4365/aaa5a8](https://doi.org/10.3847/1538-4365/aaa5a8)
- Paxton, B., Smolec, R., Schwab, J., et al. 2019, *ApJS*, 243, 10, doi: [10.3847/1538-4365/ab2241](https://doi.org/10.3847/1538-4365/ab2241)
- Pols, O. R., Schröder, K.-P., Hurley, J. R., Tout, C. A., & Eggleton, P. P. 1998, *MNRAS*, 298, 525, doi: [10.1046/j.1365-8711.1998.01658.x](https://doi.org/10.1046/j.1365-8711.1998.01658.x)
- Renzo, M., Ott, C. D., Shore, S. N., & de Mink, S. E. 2017, *A&A*, 603, A118, doi: [10.1051/0004-6361/201730698](https://doi.org/10.1051/0004-6361/201730698)
- Renzo, M., Zapartas, E., Justham, S., et al. 2023, *ApJL*, 942, L32, doi: [10.3847/2041-8213/aca4d3](https://doi.org/10.3847/2041-8213/aca4d3)
- Riley, J., Agrawal, P., Barrett, J. W., et al. 2022, *ApJS*, 258, 34, doi: [10.3847/1538-4365/ac416c](https://doi.org/10.3847/1538-4365/ac416c)
- Sana, H., de Mink, S. E., de Koter, A., et al. 2012, *Science*, 337, 444, doi: [10.1126/science.1223344](https://doi.org/10.1126/science.1223344)
- Sanyal, D., Grassitelli, L., Langer, N., & Bestenlehner, J. M. 2015, *A&A*, 580, A20, doi: [10.1051/0004-6361/201525945](https://doi.org/10.1051/0004-6361/201525945)
- Smith, N. 2014, *ARA&A*, 52, 487, doi: [10.1146/annurev-astro-081913-040025](https://doi.org/10.1146/annurev-astro-081913-040025)
- Stevenson, S., Vigna-Gómez, A., Mandel, I., et al. 2017, *Nature Communications*, 8, 14906, doi: [10.1038/ncomms14906](https://doi.org/10.1038/ncomms14906)
- van den Heuvel, E. P. J. 1969, *AJ*, 74, 1095, doi: [10.1086/110909](https://doi.org/10.1086/110909)
- Van Rossum, G., & Drake, F. L. 2009, *Python 3 Reference Manual* (Scotts Valley, CA: CreateSpace)
- van Son, L. A. C., de Mink, S. E., Renzo, M., et al. 2022, *ApJ*, 940, 184, doi: [10.3847/1538-4357/ac9b0a](https://doi.org/10.3847/1538-4357/ac9b0a)
- Vigna-Gómez, A., Neijssel, C. J., Stevenson, S., et al. 2018, *MNRAS*, 481, 4009, doi: [10.1093/mnras/sty2463](https://doi.org/10.1093/mnras/sty2463)
- Wagg, T., Broekgaarden, F., & Gültekin, K. 2024, *TomWagg/software-citation-station: v1.2, v1.2*, Zenodo, doi: [10.5281/zenodo.13225824](https://doi.org/10.5281/zenodo.13225824)
- Wagg, T., & Broekgaarden, F. S. 2024, *arXiv e-prints*, arXiv:2406.04405. <https://arxiv.org/abs/2406.04405>
- Xin, C., Renzo, M., & Metzger, B. D. 2022, *MNRAS*, 516, 5816, doi: [10.1093/mnras/stac2551](https://doi.org/10.1093/mnras/stac2551)